This is the accepted manuscript made available via CHORUS. The article has been published as:

Cyclic ferroelectric switching and quantized charge transport in math xmlns="http://www.w3.org/1998/Math/MathML">mrow>msub>mi>CuInP/mi>mn>2/mn>/msub>msub>mi mathvariant="normal">S/mi>mn>6/mn>/msub>/mrow>/math>

Daniel Seleznev, Sobhit Singh, John Bonini, Karin M. Rabe, and David Vanderbilt

Phys. Rev. B **108**, L180101 — Published 8 November 2023

DOI: 10.1103/PhysRevB.108.L180101

Cyclic Ferroelectric Switching and Quantized Charge Transport in $CuInP_2S_6$

Daniel Seleznev,[1] Sobhit Singh,[2,3] John Bonini,[4] Karin M. Rabe,[1] and David Vanderbilt[1]

[1] *Department of Physics and Astronomy, Center for Materials Theory, Rutgers University, Piscataway, New Jersey 08854, USA*
[2] *Department of Mechanical Engineering, University of Rochester, Rochester, New York 14627, USA*
[3] *Materials Science Program, University of Rochester, Rochester, New York 14627, USA*
[4] *Center for Computational Quantum Physics, Flatiron Institute, 162 5th Avenue, New York, New York 10010, USA*

The van der Waals layered ferroelectric $CuInP_2S_6$ has been found to exhibit a variety of intriguing properties arising from the fact that the Cu ions are unusually mobile in this system. While the polarization switching mechanism is usually understood to arise from Cu ion motion within the monolayers, a second switching path involving Cu motion across the van der Waals gaps has been suggested. In this work, we perform zero-temperature first-principles calculations on such switching paths, focusing on two types that preserve the periodicity of the primitive unit cell: "cooperative" paths preserving the system's glide mirror symmetry, and "sequential" paths in which the two Cu ions in the unit cell move independently of each other. We find that $CuInP_2S_6$ features a rich and varied energy landscape, and that sequential paths are clearly favored energetically both for cross-gap and through-layer paths. Importantly, these segments can be assembled to comprise a globally insulating cycle with the out-of-plane polarization evolving by a quantum as the Cu ions shift to neighboring layers. In this sense, we argue that $CuInP_2S_6$ embodies the physics of a quantized adiabatic charge pump.

$CuInP_2S_6$ (CIPS) is a van der Waals (vdW) layered ferroelectric (FE) that has drawn much attention in recent years due to its unique properties and promise for application [1–3]. Much of the interest in CIPS has been driven by its ability to maintain stable ferroelectricity in the 2D limit [4] without resorting to extrinsic mechanisms such as strain [5–7] or compensation charges [8]. However, other claimed or observed intriguing properties, such as negative longitudinal piezoelectricity [9–11] and negative capacitance [12, 13], have further motivated the investigation of this system.

The Cu ions play a central role in the physics of CIPS. First and foremost, the low-temperature FE phase results from a Cu off-centering instability at $T_c \sim 310$ K [14, 15]. Furthermore, under applied strain, the ferroelectricity in CIPS exhibits a quadruple-well potential for out-of-plane (OOP) Cu displacements [10]. That is, there are two additional high-polarization (HP) states, associated with the strain-induced appearance of stable Cu positions just inside the vdW gaps. Both the low polarization (LP) and HP states feature large, Å-scale spontaneous polar displacements, and the +LP and +HP (and −LP and −HP) states are separated by a small, strain-tunable energy barrier. Finally, at higher temperatures, Cu ionic conductivity is observed, with the onset temperature in fact even below the FE transition [16–21].

The principal "up-down" polarization switching mechanism in CIPS involves the movement of Cu ions within the monolayers, corresponding to the off-centering instability mentioned above [10, 11, 17, 22]. However, the high-temperature ionic conductivity also suggests the possibility of a novel switching pathway involving Cu ion migration across the vdW gaps, as supported by some experimental studies [12, 16, 23, 24]. Previous first-principles theoretical studies first considered a "synchronous" cross-gap switching pathway in which the primitive-cell periodicity and equivalence of the layers was preserved [12], although the structural evolution along the switching path was not reported in detail. Subsequent work by the same group considered "asynchronous" mechanisms instead, using an 8×8 in-plane supercell geometry to study processes in which Cu ions jump one at a time from a given layer to its neighbor [13]. The evolution of the OOP polarization was discussed in these works [12, 13], although the interpretation in the synchronous case was later revised [25].

The energy landscape of CIPS is quite complex, allowing for the possibility of a variety of competing paths. In this paper, we take a systematic approach focusing on the identification of synchronous switching pathways. That is, we constrain the system to retain the periodicity of the primitive 20-atom unit cell, and use zero-temperature first-principles calculations to search for low-energy pathways allowing both Cu atoms to cross the vdW gaps into adjacent layers. The characterization of such pathways is an important preliminary to understanding the switching that can occur at higher temperature, which typically involves domain wall propagation.

While we do find a path in which the Cu ions in both layers move cooperatively, it involves a rather high energy barrier. Instead, a much lower barrier is achieved by a path that allows for the sequential movement of the Cu ions, a possibility not considered in the earlier work [10, 12, 13]. This path includes multiple saddle points and local minima corresponding to different local Cu chemical environments. We also identify sequential movement as being energetically favorable for through-layer switching. The system remains robustly insulating

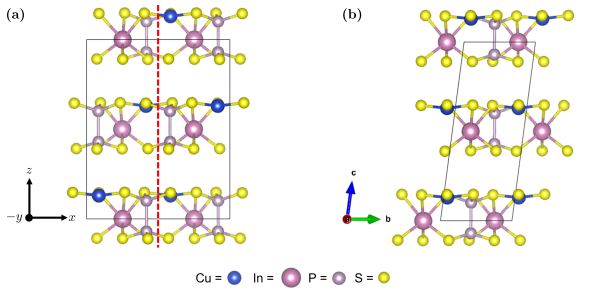


FIG. 1. (a) P^+ polar phase of CIPS in the conventional cell setting. (b) Same, but in the primitive unit cell setting. The Cu ions reside inside the monolayers and above the monolayer midplanes. The dashed red line in (a) indicates the glide mirror plane of the system. The lattice parameters and cell angles are $a = b = 6.11$ Å, $c = 13.36$ Å and $\alpha = \beta = 85.67°$, $\gamma = 120.0°$.

everywhere along both sequential switching paths, which together form a cycle transporting each Cu ion from one layer to the next. The computed change of Berry-phase polarization along this cycle corresponds to the transport of a single unit of charge by one lattice vector. The overall process is thus a FE switching cycle that embodies a quantized adiabatic charge pump [26] accomplished by ionic transport [27]. Prior works have explored this phenomenon in ionic conductors exhibiting ferroelectricity, but with the material systems considered featuring ionic vacancies [28, 29].

CIPS is a layered vdW system that is a member of the transition metal thiophosphate family, in which metal cations are found embedded in a lattice framework of $(P_2S_6)^{4-}$ anions. With two monolayers per primitive cell, the individual layers of CIPS are coupled to each other by weak vdW forces, and feature Cu^{1+} and In^{3+} cations surrounded by sulfur octahedra, with P-P dimers filling the octahedral voids (see Fig. 1). At the Curie temperature $T_c \sim 310$ K, CIPS undergoes a first order order-disorder paraelectric (PE) to FE transition, accompanied by a space-group symmetry reduction from $C2/c \rightarrow Cc$ [14, 15, 30].

Below T_c, the nominal centrosymmetric structure is unstable to a Cu off-centering instability [14, 15], with the Cu ions consequently occupy locations above or below the center planes of the monolayers, corresponding to two configurations that we denote as P^+ and P^- for "up" and "down" OOP polarization, respectively [14, 30, 31]. The former is shown in Fig. 1. However, because we shall consider cross-gap and cyclic evolution shortly, we emphasize that these labels denote the location of a Cu ion relative to its current host layer, and not to the sign of polarization in any global sense.

Importantly, both the high- and low-symmetry monoclinic space groups share a glide mirror symmetry $\{M_x|\mathbf{c}/2\}$, which maps the Cu ion in one layer onto the one in the neighboring layer. Thus, any polarization switching path that preserves the glide mirror symmetry will involve cooperative motion of both Cu ions.

In the language of the Berry-phase theory [32], on such a path the system must pass through a state in which the formal OOP polarization is either zero or half of the quantum. This may occur because the state in question has some additional symmetry, such as inversion, that enforces these values. The aforementioned $C2/c$ centrosymmetric structure corresponding to the nominal PE phase is one such example. Other $C2/c$-symmetric structures occur when both Cu ions reside at inversion centers located in the midplanes of the vdW gaps. For future reference, we also note that $C2/c$ features two subgroups, namely $P\bar{1}$ and $C2$, that while breaking glide mirror symmetry, still ensure a vanishing OOP polarization.

Our search for such cooperative switching paths is carried out using standard density-functional theory methods as detailed in the Supplemental Material [33] (SM; see also Refs. [34–41] therein), and proceeds as follows. By Δ_c we denote the difference between the Cu and In internal coordinates along the **c** lattice vector (note that Δ_c is defined modulo 1/2). Starting with the P^+ state, where $\Delta_c = 0.13$, the Cu sublattice is first incrementally shifted downward along **c** toward the nominal centrosymmetric PE structure at $\Delta_c = 0$. At each step the lattice vectors and internal coordinates are relaxed within the Cc space group subject to the Δ_c constraint. This procedure terminates by converging on the expected $C2/c$ structure when Δ_c reaches zero. The structural energy of the system increases monotonically along this path, reaching 0.72 eV for the final $C2/c$ structure, where we report all structural energies relative to that of the $P^{\pm}$ ground states on a per-unit-cell basis.

The same procedure is then repeated in the opposite direction as Δ_c is increased toward 0.25, the nominal value for Cu atoms centered in the vdW gap. The energy again increases monotonically, but this time we are surprised to find that the system remains in the Cc space group up to and including the terminal structure. We label this structure as M^+ and find its energy to be 0.97 eV. We also perform the same set of calculations starting from P^- at $\Delta_c = -0.13$, stopping this time after Δ_c is increased to 0 or decreased to -0.25. The resulting structures are found to be inversion images of those found above, with opposite sign of Δ_c and identical energies. We denote the structure at $\Delta_c = -0.25$ as M^-. The full energy profile as a function of Δ_c is depicted in the SM [33].

Although M^- and M^+ feature identical energies and are inversion images of each other, we crucially find that the structures are distinct, as is evident from the second and fourth panels of Fig. 2(a). While the Cu ions see a roughly tetrahedral environment in both cases, three of the four bonds are to S atoms in the lower layer for M^+, and the reverse is true for the M^-. As a result, a continuous path across the vdW gap is not yet identified.

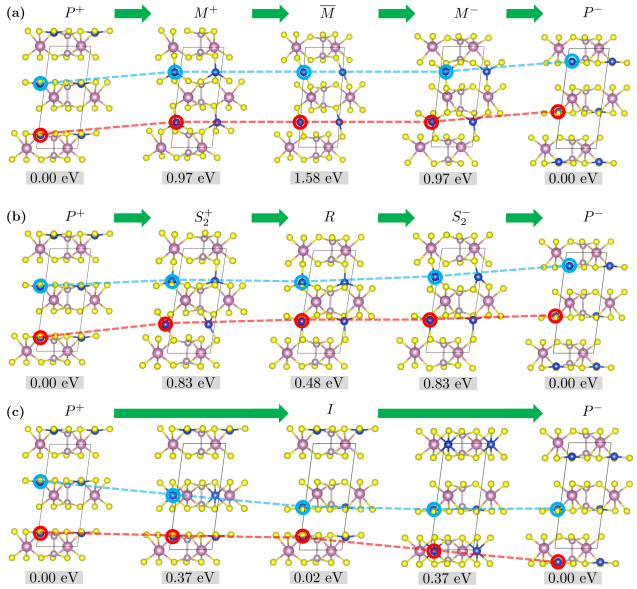


FIG. 2. (a) The representative sequence $P^+ \to M^+ \to \overline{M} \to M^- \to P^-$. The Cu ions in the lower (red) and upper (blue) layers of the unit cell move cooperatively along the **c** lattice vector throughout the switching path, as emphasized by the guiding lines. (b) The representative sequence $P^+ \to S_2^+ \to R \to S_2^- \to P^-$. The lower Cu ions move across the vdW gap first, and are subsequently followed by the Cu ions in the upper vdW gap. (c) Sequence of structures from P^+ to P^- passing through I in the middle. The upper Cu ions move through a monolayer first, followed by the bottom Cu ions. The number below a structure indicates its energy relative to $P^\pm$.

To complete the cross-gap cooperative switching path, we perform a series of nudged elastic band (NEB) calculations, detailed in the SM [33], from which we find that the midpoint of the cross-gap path, which we designate as $\overline{M}$, is a structure with $C2/c$ symmetry. The full sequence $P^+ \to M^+ \to \overline{M} \to M^- \to P^-$ is illustrated in the five panels of Fig. 2(a), highlighting the cooperative nature of Cu motion along the **c** lattice vector. In passing along this path, the Cu ions visit a variety of coordination environments. The Cu ions begin in a nearly trigonal planar setting (P^+), then pass through the distorted tetrahedral coordination environment (M^+) mentioned above, before reaching the midpoint of the switching path ($\overline{M}$) where a linear two-fold coordination appears. On the second half of the path, the Cu ions pass through the same environments but in reverse. The energy barrier for the switching path is defined by $\overline{M}$, and is found to be 1.58 eV. Such a high barrier suggests that this switching path is implausible, and that alternative paths should be investigated.

The $\overline{M}$ structure is found to have two unstable phonon modes. Unsurprisingly, one mode corresponds to the tangent to the NEB path as it passes over the barrier; this is a polar B_u mode that reduces the symmetry from $C2/c$ to Cc. However, the second A_u mode reduces the symmetry from $C2/c$ to $C2$, and features one Cu ion continuing on into the vdW gap, while the second Cu recedes back towards its original layer. The existence of this second unstable mode suggests a new switching path featuring sequential Cu motion, in which the two Cu ions in the primitive cell traverse the vdW gaps one at a time.

To explore such sequential paths, we distort the $\overline{M}$ structure along the A_u mode and perform a full structural relaxation within $C2$; we obtain the structure we refer to as R, depicted in the middle panel of Fig. 2(b). The figure illustrates that unlike the previously considered structures, R features Cu ions doubly occupying half of the layers, while leaving the other half empty [42]. We find that R has no unstable zone center phonon modes, eliminating it as a barrier candidate.

To identify possible barriers, we perform an NEB path search initialized with the linearly interpolated path between P^+ and R, keeping the initial lattice vectors of each structure fixed during the calculation. However, we find that the calculation is difficult to converge because of the complexity of the path, which appears to pass over multiple saddle points on the way from P^+ to R.

To circumvent this difficulty, we resort to a two-stage procedure in which we first identify these saddle points in the energy landscape using a direct saddle-point search technique known as the dimer method [43, 44]. In this way we identify two saddle points which we refer to as S_1^+ and S_2^+, the latter of which is shown in the second panel of Fig. 2(b). These are then used as anchor points to split our NEB path into three segments $P^+ \to S_1^+$, $S_1^+ \to S_2^+$, and $S_2^+ \to R$, and a separate NEB calculation for each segment is initialized with a linear interpolation of internal coordinates and lattice vectors between the respective endpoints. During the calculations, the initial lattice vectors of each structure on the NEB paths are held fixed.

The portion of the switching path from R to P^- is related to that from $P^+ \to R$ by a C_{2x} rotation symmetry. The structures with the highest energy are $S_1^\pm$, leading to an energy barrier of 0.91 eV, much lower than the $\overline{M}$ barrier of 1.58 eV reported above. Representative structures on the switching path are shown in Fig. 2(b). The Cu ions are found to pass through tetrahedral and coplanar trigonal local coordination environments, but never linear ones as was the case for the cooperative switching path shown in Fig. 2(a). Importantly, we emphasize that, unlike for the previous path, the Cu motion across the vdW gap is now sequential. That is, the Cu in the lower half of the primitive cell moves across the vdW gap first in Fig. 2(b), and only then does the second Cu traverse the upper vdW gap.

The fact that the favored switching path through the vdW gaps is a sequential one raises the question of whether the same might be true of the "ordinary" switching path from P^- to P^+, in which the Cu ions move

within the monolayers [22]. To investigate this, we identify the unstable zone center phonon modes of the PE phase structure residing at the midpoint of the through-layer cooperative switching path. Two modes are found: a polar B_u mode corresponding to the Cu off-centering instability driving the transition to the FE phase, and an antipolar B_g mode that reduces the symmetry to $P\bar{1}$. We distort the PE structure along the B_g mode, and relax the distorted structure within $P\bar{1}$ while preserving the 20-atom translational symmetry of the PE phase. The resulting centrosymmetric structure, denoted as I, is metastable (having no unstable zone-center modes) and features an energy of only 0.02 eV relative to $P^{\pm}$.

To find the saddle points we perform an NEB calculation initialized with a linearly interpolated path between I and P^+. In the course of the calculation, the initial lattice vectors of each structure are held fixed. The calculation reveals an energy barrier of 0.37 eV, which is much lower than the 0.72 eV value reported above for cooperative switching through the layer. The path $P^- \to I$ is obtained by an inversion of the structures residing on $I \to P^+$.

Fig. 2(c) illustrates some of the representative structures on the switching path from P^+ to P^- passing through I. As in the cross-gap switching path passing through R, the Cu ions move independently of each other. However, here they pass through the monolayers, with one Cu in the primitive cell initially passing through a layer followed by the second.

Note that we found, first for cross-gap switching and then for through-layer switching, that the barrier for sequential switching is only slightly more than half that of the cooperative path. We take this as strong evidence that the CIPS system is close to the order-disorder limit, as has also been argued previously by others [14, 15, 30]. In that limit, there is an energy cost for a layer to switch, independent of its neighbors [45]. In the displacive limit, instead, one would expect that the sequential barrier would be much higher in energy, or even that the intermediate metastable antipolar state might well be eliminated entirely.

The combination of the $P^+ \to R \to P^-$ and $P^- \to I \to P^+$ switching paths described above yields a full cycle that brings P^+ back to itself, but with every Cu ion having moved vertically into the adjacent layer above. We would therefore like to understand the evolution of the OOP electric polarization along this cycle. This is only possible if the system remains insulating all along the path. Crucially, we find that it does, with the smallest direct or indirect band gap of 0.88 eV being found at the structures corresponding to $p_3 = 0.46$ and 0.54 in Fig. 3. Since we are primarily interested in the polarization normal to the layers, we compute the reduced electric polarization $p_3 = V_{\text{cell}}\mathbf{b}_3 \cdot \mathbf{P}/2\pi$ for each NEB-generated configuration along the path. Here V_{cell} is the unit cell volume, $\mathbf{b}_3$ is the third reciprocal lattice vector, and $\mathbf{P}$ is the Berry-phase polarization. Note that p_3 is defined only modulo a quantum of elementary charge e.

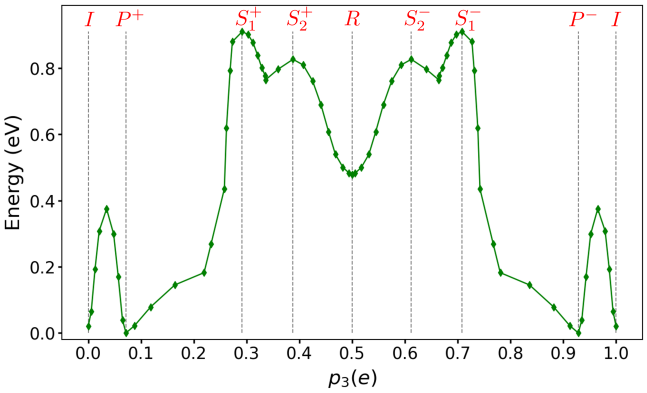


FIG. 3. The full NEB energy profile of the combined sequential switching paths plotted versus the reduced polarization p_3. The most significant energy barriers for switching are defined by $S_1^{\pm}$ (cross-gap), and the local maxima on the $P^{\pm} \to I$ paths (through-layer).

Figure 3 presents the total energy of each structure along the cycle on the vertical axis, and their corresponding calculated reduced layer-normal polarizations p_3 on the horizontal axis. First, we note that the polarization remains well defined and increases monotonically along the cycle. Moreover, we see that at the completion of the path, the polarization has changed by a quantum. The formal oxidation state of Cu in this compound is Cu^{1+}, consistent with the fact that one Cu ion from each primitive cell has moved into the vertically adjacent cell, thus realizing quantized charge transport [27–29].

This path's existence suggests the possibility of adiabatic charge transport in this system. An ideal scenario would be one in which a combination of two or more parameters, such as strain components or external fields, could be manipulated to carry the system deterministically along such a path, thereby realizing an adiabatic charge pump [46].

Having specified our switching path, we would also like to obtain an order-of-magnitude estimate of the coercive fields involved in the switching. Ideally this could be done by using finite-field methods to follow the electric equation of state in the form of energy E as a function of OOP polarization P_z [47–49], and associating the coercive field with the maximum of dE/dP_z along the switching path. Since we are only interested in rough estimates here, we instead simply compute the finite difference $\Delta E/\Delta P_z$ on the most relevant segments of the switching path. Referring to Fig. 3, we find values of 0.77, 0.24, and 0.77 V/Å in going from the minimum to the saddle point along I towards P^+, along R towards S_2^-, and along P^- towards I, respectively. For the path from P^+ towards S_1^+ the finite difference is taken to start from the point at $p_3 = 0.26$, yielding a value of 1.21 V/Å. It is notewor-

thy that this latter coercive field for switching through the vdW gap does not greatly exceed those required for switching through the layers.

First-principles predictions of coercive fields based on preserving primitive cell periodicity often overestimate experimentally measured values by as much as two orders of magnitude. This is unsurprising given that such calculations exclude switching via domain-wall nucleation and motion and ignore the effects of temperature and disorder. In this context, our values, while high compared to corresponding values for conventional FEs, are not far out of line with experimental values for CIPS in the range of 10^{-4} to 10^{-3} V/Å [14, 16], which are also high compared with experimental coercive fields of conventional FEs.

To summarize, we investigated the energy landscape of CIPS to identify polarization switching paths involving either cooperative Cu ion motion preserving the system's glide mirror symmetry, or sequential Cu motion. Aside from the nature of the Cu motion, the two switching paths are distinguished by the local coordination environments that the Cu ions visit in the course of the switching. The sequential switching paths through the monolayers and vdW gaps lead to significantly smaller energy barriers than their respective cooperative counterparts. Since all structures on the sequential switching paths remain insulating, we argue that the combination of the two paths leads to a FE switching cycle embodying the physics of a quantized adiabatic charge pump. Finally, we perform an order-of-magnitude estimate of the coercive fields needed to drive the system across the most significant energy barriers along the sequential switching cycle, and find that they are comparable in magnitude.

Our findings reinforce an emerging focus on a class of materials that simultaneously exhibit ferroelectricity and ionic conductivity in the bulk. In most systems, ionic transport is associated with the degradation of the FE state, and relatively few systems are known in which the two coexist [50–56]. Our study offers an indication that this class of materials has the potential to exhibit unusually rich behavior. Much remains to be understood, and further research is needed, regarding the relationship of ferroelectricity and ionic conductivity in these intriguing materials [16, 57–59].

DS and DV acknowledge support from the National Science Foundation under grants DGE-1842213 and DMR-1954856, respectively. KMR and SS acknowledge support from Office of Naval Research Grant N00014-21-1-2107, and JB acknowledges support from the Simons Foundation. SS acknowledges support from the University Research Awards at the University of Rochester.

[1] Fei Xue, Jr-Hau He, and Xixiang Zhang, "Emerging van der Waals ferroelectrics: Unique properties and novel devices," Applied Physics Reviews **8**, 021316 (2021).
[2] Dawei Zhang, Peggy Schoenherr, Pankaj Sharma, and Jan Seidel, "Ferroelectric order in van der Waals layered materials," Nature Reviews Materials **8**, 25–40 (2023).
[3] Shuang Zhou, Lu You, Hailin Zhou, Yong Pu, Zhigang Gui, and Junling Wang, "Van der Waals layered ferroelectric $CuInP_2S_6$: Physical properties and device applications," Frontiers of Physics **16**, 13301 (2020).
[4] Fucai Liu, Lu You, Kyle L. Seyler, Xiaobao Li, Peng Yu, Junhao Lin, Xuewen Wang, Jiadong Zhou, Hong Wang, Haiyong He, Sokrates T. Pantelides, Wu Zhou, Pradeep Sharma, Xiaodong Xu, Pulickel M. Ajayan, Junling Wang, and Zheng Liu, "Room-temperature ferroelectricity in $CuInP_2S_6$ ultrathin flakes," Nature Communications **7**, 12357 (2016).
[5] K. J. Choi, M. Biegalski, Y. L. Li, A. Sharan, J. Schubert, R. Uecker, P. Reiche, Y. B. Chen, X. Q. Pan, V. Gopalan, L.-Q. Chen, D. G. Schlom, and C. B. Eom, "Enhancement of ferroelectricity in strained $BaTiO_3$ thin films," Science **306**, 1005–1009 (2004).
[6] V. Garcia, S. Fusil, K. Bouzehouane, S. Enouz-Vedrenne, N. D. Mathur, A. Barthélémy, and M. Bibes, "Giant tunnel electroresistance for non-destructive readout of ferroelectric states," Nature **460**, 81–84 (2009).
[7] Yajun Zhang, Gui-Ping Li, Takahiro Shimada, Jie Wang, and Takayuki Kitamura, "Disappearance of ferroelectric critical thickness in epitaxial ultrathin $BaZrO_3$ films," Phys. Rev. B **90**, 184107 (2014).
[8] Na Sai, Alexie M. Kolpak, and Andrew M. Rappe, "Ferroelectricity in ultrathin perovskite films," Phys. Rev. B **72**, 020101 (2005).
[9] Lu You, Yang Zhang, Shuang Zhou, Apoorva Chaturvedi, Samuel A. Morris, Fucai Liu, Lei Chang, Daichi Ichinose, Hiroshi Funakubo, Weijin Hu, Tom Wu, Zheng Liu, Shuai Dong, and Junling Wang, "Origin of giant negative piezoelectricity in a layered van der Waals ferroelectric," Science Advances **5**, eaav3780 (2019).
[10] John A. Brehm, Sabine M. Neumayer, Lei Tao, Andrew O'Hara, Marius Chyasnavichus, Michael A. Susner, Michael A. McGuire, Sergei V. Kalinin, Stephen Jesse, Panchapakesan Ganesh, Sokrates T. Pantelides, Petro Maksymovych, and Nina Balke, "Tunable quadruple-well ferroelectric van der Waals crystals," Nature Materials **19**, 43–48 (2020).
[11] Sabine M. Neumayer, Eugene A. Eliseev, Michael A. Susner, Alexander Tselev, Brian J. Rodriguez, John A. Brehm, Sokrates T. Pantelides, Ganesh Panchapakesan, Stephen Jesse, Sergei V. Kalinin, Michael A. McGuire, Anna N. Morozovska, Petro Maksymovych, and Nina Balke, "Giant negative electrostriction and dielectric tunability in a van der Waals layered ferroelectric," Phys. Rev. Materials **3**, 024401 (2019).
[12] Sabine M. Neumayer, Lei Tao, Andrew O'Hara, Michael A. Susner, Michael A. McGuire, Petro Maksymovych, Sokrates T. Pantelides, and Nina Balke, "The concept of negative capacitance in ionically conductive van der Waals ferroelectrics," Advanced Energy Materials **10**, 2001726 (2020).
[13] Andrew O'Hara, Nina Balke, and Sokrates T. Pantelides,

"Unique features of polarization in ferroelectric ionic conductors," Advanced Electronic Materials **8**, 2100810 (2022).
[14] V. Maisonneuve, V. B. Cajipe, A. Simon, R. Von Der Muhll, and J. Ravez, "Ferrielectric ordering in lamellar $CuInP_2S_6$," Phys. Rev. B **56**, 10860–10868 (1997).
[15] Yu. M. Vysochanskii, V. A. Stephanovich, A. A. Molnar, V. B. Cajipe, and X. Bourdon, "Raman spectroscopy study of the ferrielectric-paraelectric transition in layered $CuInP_2S_6$," Phys. Rev. B **58**, 9119–9124 (1998).
[16] Shuang Zhou, Lu You, Apoorva Chaturvedi, Samuel A. Morris, Jason S. Herrin, Na Zhang, Amr Abdelsamie, Yuzhong Hu, Jieqiong Chen, Yang Zhou, Shuai Dong, and Junling Wang, "Anomalous polarization switching and permanent retention in a ferroelectric ionic conductor," Mater. Horiz. **7**, 263–274 (2020).
[17] Nina Balke, Sabine M. Neumayer, John A. Brehm, Michael A. Susner, Brian J. Rodriguez, Stephen Jesse, Sergei V. Kalinin, Sokrates T. Pantelides, Michael A. McGuire, and Petro Maksymovych, "Locally controlled Cu-ion transport in layered ferroelectric $CuInP_2S_6$," ACS Applied Materials & Interfaces **10**, 27188–27194 (2018).
[18] V. Maisonneuve, J. M. Reau, Ming Dong, V. B. Cajipe, C. Payen, and J. Ravez, "Ionic conductivity in ferroic $CuInP_2S_6$ and $CuCrP_2S_6$," Ferroelectrics **196**, 257–260 (1997).
[19] J. Banys, J. Macutkevic, V. Samulionis, A. Brilingas, and Yu. Vysochanskii, "Dielectric and ultrasonic investigation of phase transition in $CuInP_2S_6$ crystals," Phase Transitions **77**, 345–358 (2004).
[20] Andrius Dziaugys, Juras Banys, Jan Macutkevic, and Yulian Vysochanskii, "Anisotropy effects in thick layered $CuInP_2S_6$ and $CuInP_2Se_6$ crystals," Phase Transitions **86**, 878–885 (2013).
[21] Jan Macutkevic, Juras Banys, and Yulian Vysochanskii, "Electrical conductivity of layered $CuInP_2(S_xSe_{1-x})_6$ crystals," physica status solidi (b) **252**, 1773–1777 (2015).
[22] Sabine N. Neal, Sobhit Singh, Xiaochen Fang, Choongjae Won, Fei-Ting Huang, Sang-Wook Cheong, Karin M. Rabe, David Vanderbilt, and Janice L. Musfeldt, "Vibrational properties of $CuInP_2S_6$ across the ferroelectric transition," Phys. Rev. B **105**, 075151 (2022).
[23] Sabine M. Neumayer, Lei Tao, Andrew O'Hara, John Brehm, Mengwei Si, Pai-Ying Liao, Tianli Feng, Sergei V. Kalinin, Peide D. Ye, Sokrates T. Pantelides, Petro Maksymovych, and Nina Balke, "Alignment of polarization against an electric field in van der Waals ferroelectrics," Phys. Rev. Applied **13**, 064063 (2020).
[24] Dawei Zhang, Zheng-Dong Luo, Yin Yao, Peggy Schoenherr, Chuhan Sha, Ying Pan, Pankaj Sharma, Marin Alexe, and Jan Seidel, "Anisotropic ion migration and electronic conduction in van der Waals ferroelectric $CuInP_2S_6$," Nano Letters **21**, 995–1002 (2021).
[25] Sabine M. Neumayer, Lei Tao, Andrew O'Hara, Michael A. Susner, Michael A. McGuire, Petro Maksymovych, Sokrates T. Pantelides, and Nina Balke, "The concept of negative capacitance in ionically conductive van der Waals ferroelectrics," Advanced Energy Materials **11**, 2103493 (2021).
[26] D. J. Thouless, "Quantization of particle transport," Phys. Rev. B **27**, 6083–6087 (1983).
[27] Lai Jiang, Sergey V. Levchenko, and Andrew M. Rappe, "Rigorous definition of oxidation states of ions in solids," Phys. Rev. Lett. **108**, 166403 (2012).
[28] Menghao Wu, J. D. Burton, Evgeny Y. Tsymbal, Xiao Cheng Zeng, and Puru Jena, "Hydroxyl-decorated graphene systems as candidates for organic metal-free ferroelectrics, multiferroics, and high-performance proton battery cathode materials," Phys. Rev. B **87**, 081406 (2013).
[29] Xuechen Wang, Yangyang Ren, and Menghao Wu, "Unconventional ferroelectricity with quantized polarizations in ionic conductors: High-throughput screening," The Journal of Physical Chemistry Letters **13**, 9552–9557 (2022).
[30] A. Simon, J. Ravez, V. Maisonneuve, C. Payen, and V. B. Cajipe, "Paraelectric-ferroelectric transition in the lamellar thiophosphate $CuInP_2S_6$," Chemistry of Materials **6**, 1575–1580 (1994).
[31] V. Maisonneuve, M. Evain, C. Payen, V.B. Cajipe, and P. Molinié, "Room-temperature crystal structure of the layered phase $Cu^{I}In^{III}P_2S_6$," Journal of Alloys and Compounds **218**, 157–164 (1995).
[32] Raffaele Resta and David Vanderbilt, "Theory of polarization: A modern approach," in *Physics of Ferroelectrics: A Modern Perspective* (Springer Berlin Heidelberg, Berlin, Heidelberg, 2007) pp. 31–68.
[33] See Supplemental Material *[URL to be inserted by publisher]* for computational details, a description of how we identified $\overline{M}$, and a plot of energy against Δ_c for the cooperative switching paths. We include files for the structures corresponding to the points in Fig. 3 of the main text and Fig. 1 of the Supplemental Material. We also include a structural animation of the cycle depicted in Fig. 3 of the main text.
[34] G. Kresse and J. Furthmüller, "Efficient iterative schemes for *ab initio* total-energy calculations using a plane-wave basis set," Phys. Rev. B **54**, 11169–11186 (1996).
[35] G. Kresse and D. Joubert, "From ultrasoft pseudopotentials to the projector augmented-wave method," Phys. Rev. B **59**, 1758–1775 (1999).
[36] John P. Perdew, Kieron Burke, and Matthias Ernzerhof, "Generalized gradient approximation made simple," Phys. Rev. Lett. **77**, 3865–3868 (1996).
[37] Stefan Grimme, Jens Antony, Stephan Ehrlich, and Helge Krieg, "A consistent and accurate ab initio parametrization of density functional dispersion correction (DFT-D) for the 94 elements H-Pu," The Journal of Chemical Physics **132**, 154104 (2010).
[38] Greg Mills and Hannes Jónsson, "Quantum and thermal effects in H_2 dissociative adsorption: Evaluation of free energy barriers in multidimensional quantum systems," Phys. Rev. Lett. **72**, 1124–1127 (1994).
[39] Gregory Mills, Hannes Jónsson, and Gregory K. Schenter, "Reversible work transition state theory: application to dissociative adsorption of hydrogen," Surface Science **324**, 305–337 (1995).
[40] Hannes Jónsson, Greg Mills, and Karsten W. Jacobsen, "Nudged elastic band method for finding minimum energy paths of transitions," in *Classical and Quantum Dynamics in Condensed Phase Simulations*, pp. 385–404.
[41] R. D. King-Smith and David Vanderbilt, "Theory of polarization of crystalline solids," Phys. Rev. B **47**, 1651–1654 (1993).
[42] Note1, The 2-fold rotation axis of R is found to lie along x and to pass through the monolayer midplanes.
[43] Graeme Henkelman and Hannes Jónsson, "A dimer

method for finding saddle points on high dimensional potential surfaces using only first derivatives," The Journal of Chemical Physics **111**, 7010–7022 (1999).

[44] Andreas Heyden, Alexis T. Bell, and Frerich J. Keil, "Efficient methods for finding transition states in chemical reactions: Comparison of improved dimer method and partitioned rational function optimization method," The Journal of Chemical Physics **123**, 224101 (2005).

[45] Note2, In the order-disorder limit, an enlarged supercell in which only one layer switches would appear to require a lower barrier on an energy-per-unit-volume basis, but in this limit an energy-per-layer basis is more relevant.

[46] Note3, In the present case the barriers still appear to be too large to make this plausible, but further research is clearly desirable to see if more promising related systems can be found.

[47] Oswaldo Diéguez and David Vanderbilt, "First-principles calculations for insulators at constant polarization," Phys. Rev. Lett. **96**, 056401 (2006).

[48] Massimiliano Stengel, Nicola A. Spaldin, and David Vanderbilt, "Electric displacement as the fundamental variable in electronic-structure calculations," Nature Physics **5**, 304–308 (2009).

[49] Massimiliano Stengel, David Vanderbilt, and Nicola A. Spaldin, "First-principles modeling of ferroelectric capacitors via constrained displacement field calculations," Phys. Rev. B **80**, 224110 (2009).

[50] F. Habbal, J. A. Zvirgzds, and J. F. Scott, "Raman spectroscopy of structural phase transitions in $Ag_{26}I_{18}W_4O_{16}$," The Journal of Chemical Physics **69**, 4984–4989 (1978).

[51] J. F. Scott, F. Habbal, and J. A. Zvirgzds, "Ferroelectric phase transition in the superionic conductor $Ag_{26}I_{18}W_4O_{16}$," The Journal of Chemical Physics **72**, 2760–2762 (1980).

[52] S. Hoshino, H. Fujishita, M. Takashige, and T. Sakuma, "Phase transition of Ag_3SX (X=I, Br)," Solid State Ionics **3-4**, 35–39 (1981).

[53] S. Yu. Stefanovich, V. B. Kalinin, and A. Nogai, "Ferroelectric-superionic conductor phase transitions in $Na_3Sc_2(PO_4)_3$ and ITS isomorphes," Ferroelectrics **55**, 325–328 (1984).

[54] S. Yu. Stefanovich, V. K. Yanovsky, A. V. Astafyev, V. I. Voronkova, and Yu. N. Venevtsev, "Ferroelectric-superionic conductor phase transitions in crystals $MeNbWO_6{\cdot}nH_2O$ (Me=Tl, Rb)," Japanese Journal of Applied Physics **24**, 373 (1985).

[55] A. I. Baranov, V. P. Khiznichenko, and L. A. Shuvalov, "High temperature phase transitions and proton conductivity in some kdp-family crystals," Ferroelectrics **100**, 135–141 (1989).

[56] J.F. Scott, "A comparison of Ag- and proton-conducting ferroelectrics," Solid State Ionics **125**, 141–146 (1999).

[57] Sabine M. Neumayer, Mengwei Si, Junkang Li, Pai-Ying Liao, Lei Tao, Andrew O'Hara, Sokrates T. Pantelides, Peide D. Ye, Petro Maksymovych, and Nina Balke, "Ionic control over ferroelectricity in 2D layered van der Waals capacitors," ACS Applied Materials & Interfaces **14**, 3018–3026 (2022).

[58] Gustav Lindgren, Anton Ievlev, Stephen Jesse, Olga S. Ovchinnikova, Sergei V. Kalinin, Rama K. Vasudevan, and Carlota Canalias, "Elasticity modulation due to polarization reversal and ionic motion in the ferroelectric superionic conductor $KTiOPO_4$," ACS Applied Materials & Interfaces **10**, 32298–32303 (2018).

[59] Mario Maglione, Anand Theerthan, Vincent Rodriguez, Alexandra Peña, Carlota Canalias, Bertrand Ménaert, and Benoît Boulanger, "Intrinsic ionic screening of the ferroelectric polarization of KTP revealed by second-harmonic generation microscopy," Opt. Mater. Express **6**, 137–145 (2016).